Master's Thesis

석사 학위논문

The Performance Analysis of Non-coherent M-ary DPSK Receiver Applying the Repetition Scheme for Low-power Communications

Seungik Cho (조 승 익 趙 承 翼)

Department of Information and Communication Engineering

정보통신융학공학전공

DGIST

2016

Master's Thesis

석사 학위논문

The Performance Analysis of Non-coherent M-ary DPSK Receiver Applying the Repetition Scheme for Low-power Communications

Seungik Cho (조 승 익 趙 承 翼)

Department of Information and Communication Engineering

정보통신융학공학전공

DGIST

2016

The Performance Analysis of Non-coherent M-ary DPSK Receiver Applying the Repetition Scheme for Low-power Communications

Advisor: Professor Ji-Woong Choi

Co-Advisor: Professor Hongsoo Choi

By

Seungik Cho

Department of Information and Communication Engineering

DGIST

A thesis submitted to the faculty of DGIST in partial fulfillment of the requirements for the degree of Master of Science in the Department of Information and Communication Engineering. The study was conducted in accordance with Code of Research Ethics[1)].

May. 31. 2016

Approved by

Professor Ji-Woong Choi _____ (Signature)

(Advisor)

Professor Hongsoo Choi _____ (Signature)

(Co-Advisor)

1) Declaration of Ethical Conduct in Research**:** I, as a graduate student of DGIST, hereby declare that I have not committed any acts that may damage the credibility of my research. These include, but are not limited to: falsification, thesis written by someone else, distortion of research findings or plagiarism. I affirm that my thesis contains honest conclusions based on my own careful research under the guidance of my thesis advisor.

The Performance Analysis of Non-coherent M-ary DPSK Receiver Applying the Repetition Scheme for Low-power Communications

Seungik Cho

Accepted in partial fulfillment of the requirements for the degree of
Master of Science

May. 31. 2016

Head of Committee_____(인)

Prof. Ji-Woong Choi

Committee Member_____(인)

Prof. Hongsoo Choi

Committee Member_____(인)

Prof. Jae-Eun Jang

MS/IC

201422018

조 승 익. Seungik Cho. The Performance Analysis of Non-coherent M-ary DPSK Receiver Applying the Repetition Scheme for Low-power Communications. 2016. 35p. Advisors Prof. Ji-Woong Choi, Prof. Co-Advisors Hongsoo Choi.

Abstract

In this paper, we analyze performance of a non-coherent M-ary differential phase shift keying (DPSK) receiver applying the repetition scheme for low-power and reliable communications. The well-known feature of a non-coherent DPSK is that significantly low complexity implementation can be achieved over coherent PSK, since there is no need of phase synchronization of the received signal, while the receiver performance becomes worse. In order to achieve robust detection performance, a repetition code with error-correction capability can be jointly employed with DPSK. For example, M-ary DPSK modulation with bit spreader and interleaver is used in IEEE 802.15.6 WBAN and IEEE P1901.2 for reliability improvement. In this paper, on the other hand, we employ the symbol repetition instead of bit repetition in order to find possibility of additional performance gain. To be specific, the error rate of a non-coherent M-ary DPSK receiver with repetition scheme is influenced by the noise distribution shape whose effect changes in accordance with a repetition order. In other words, we confirmed that when certain repetition order in each modulation order is given, a noise distribution forces a received signal to be distributed more within or outside error decision boundary. That is, our proposed scheme can be helpful in reducing the bit error rate for non-coherent M-ary DPSK with repetition. In addition to simply employing symbol repetition, an alternative that can achieve higher reliability via exploiting further information at signal demodulation is proposed. In this paper, we investigate performance of a non-coherent M-ary DPSK receiver with symbol repetition by performing the simulation and experiments. In addition, we find the repetition order which can optimize the energy efficiency of a non-coherent M-ary DPSK receiver.

Keywords: Low-power communication, Reliability, Non-coherent, Differential phase shift keying (DPSK), Symbol repetition

Contents

Ⅰ. INTRODUCTION

Low-power communication is one of the most important issue in various research area of recent and future communication technology, and related researches have been widely studied [1], [2], [3], [4], [5]. The Internet of Things (IoT) [6], [7], [8] technologies such as radio-frequency identification (RFID), wireless sensor network and near field communication, cloud computing and smart devices are up-and-coming research areas nowadays. Figure 1.1 shows the trend of rapid growth for future IoT [9].

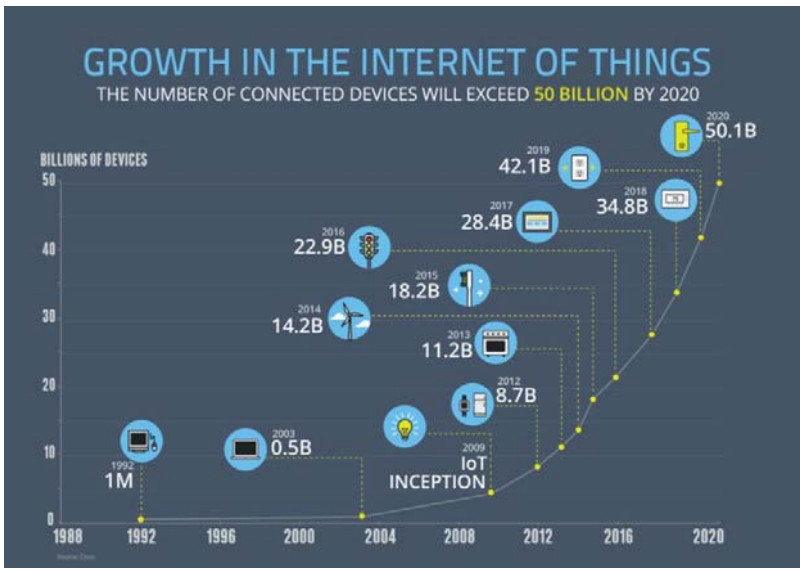

Figure 1.1 Growth in the Internet of Things

With the development of IoT technologies, smart wireless sensing devices with small size will be deployed in various application environments. Typically, these wireless sensing devices are constrained by limitations in energy resource, signal processing and communication range, storage capability and reliability, etc. [10]. Also, their operation must satisfy the real-time communication among applications under little or no direct human interactions [10]. In order to well satisfy such requirements of these wireless sensor devices, for example, monitoring the device performance or sending commands to a sensor node, it is necessary to design efficient

and reliable communication protocol to remotely manage wireless sensor nodes (WSN) without consuming significant resources. In this sense, the contribution of this work is to design a transceiver for low-power and reliable communications.

As mentioned above, WSN has significant constraints and problems such as limited power consumption and low communication reliability. There are a variety of reasons for a limited power consumption of WSNs based on IoT. Firstly, they should be very cheaply provided to consumers. Also, these devices for WSN require sufficient miniaturization in order to be seamlessly integrated virtually and able to achieve ubiquitous connectivity among persons, machines, objects and the environment [11]. Therefore, a battery of WSNs should also be miniaturized for practical implementation with highly limited capability of power such as a coin-sized battery. In addition, since a wireless sensor network consists of enormous sensor nodes (from hundreds to thousands) with massive connectivity to monitor an area to get data about the environment [12], battery replacement of WSNs within a network is quite burdensome. For example, body measurement devices that consist of the network system between implant and wearable device have some requirements. Since these devices are implanted inside human body or exteriorly attached for a long time, they must be miniaturized and need to operate for a several years without replacing a battery [13]. The miniaturization of a device limits the power consumption and thus requires low-power implementation. In the case of implanted devices, the charge of a battery is difficult inside human body and thus one can replace them only through the surgery [13]. Also, these devices might directly impact the life of the person. If the communication among devices is poor, serious patients can be in danger of death by sudden communication interruption. Hence, the low-power and reliable communication is jointly required.

The previous researches for low-power communication have mainly used frequency shift keying (FSK) and on-off keying (OOK) [14], [15], [16], [17], [18]. The differential phase shift

keying (DPSK) modulation is a non-coherent scheme that does not require perfect phase synchronization [19]. Note that the non-coherent scheme is known to be highly efficient than a coherent scheme such as quadrature amplitude modulation (QAM) and phase shift keying (PSK), since the complexity of non-coherent modulation is lower than that of coherent modulation [20]. Therefore, the DPSK modulation can be a good alternative for low power communication. As mentioned earlier, the use of OOK and FSK modulation can obtain the effect of low power consumption, but it is followed by the cost of considerable performance, i.e., low communication reliability. Although the DPSK modulation also suffers from low communication reliability, robust receiving performance can be achieved by jointly employing error correction techniques [21], [22]. For example, the IEEE P1901.2 uses the repetition scheme with DPSK or PSK modulations when the channel is poor [22], [23], and the IEEE 802.15.6 narrowband WBAN system employs the DPSK modulation with bit spreader and interleaver for reliability improvement [21]. By using a bit spreader, an input bit sequence is encoded in the manner of the repetition scheme, and the use of a bit interleaver provides robustness against error propagation. In this research, a repetition coding scheme is employed with the DPSK modulation for low-power and reliable communications, which is one of the basic forward error correction (FEC) methods. The repetition coding is to just repeat a message multiple times. At the cost of the data rate, its simplicity in encoding and decoding procedure enables low-power and higher reliability implementation through time diversity in time varying channels. Thus, the repetition scheme is accepted in a variety of communication standards.

In this work, the non-coherent M-ary DPSK with repetition scheme is found to be capable of significantly improving the DPSK system performance with proper choice of the modulation order (M) and the repetition order (R). To be specific, the de-repeated signal distribution varies in accordance with an intensity of the skewness generated due to differential characteristic of DPSK modulation with repetition scheme. In addition, with a proper choice of the repetition

order, the non-coherent DPSK with repetition scheme is shown to provide gain in performance [24]. Since some communication standards use the DPSK modulation with repetition scheme, as mentioned earlier, the contribution of this work can be helpful in improving the reliability as well as reducing the power consumption. Moreover, by exploiting a useful property of DPSK with repetition, the non-coherent M-ary DPSK with proposed scheme enables further performance improvement. In this research, this phenomenon will be investigated, and selecting the proper repetition order for performance enhancement will be discussed. The remainder of this paper is organized as follows. In Section Ⅱ, the basic concept of related work is introduced. The system model is formulated in Section Ⅲ. The effect of the received noise distribution by the skewness on error rate is described, and the method for further performance improvement is proposed in Section Ⅳ. Simulation and experimental results for performance evaluation are provided in Section Ⅴ, and Section Ⅵ concludes this paper.

II. BASIC CONCEPT OF RELATED WORK

A. Differential phase shift keying (DPSK) modulation

In this paper, a DPSK system, which is the 'non-coherent' version of PSK, is considered to use differential characteristics of DPSK with repetition scheme. The main feature of DPSK is that it eliminates the need for synchronizing the receiver to the transmitter by combining two basic operations at the transmitter, that is, the differential encoding of the input binary sequence, and the PSK modulation of the encoded sequence. Figure 2.1 shows block diagram for DPSK signal transmission. The logic network block is used to convert the raw input binary sequence $\{b_k\}$ into the differential encoded sequence $\{d_k\}$, and the one-bit delay element memory acts as the memory unit. The differential encoded sequence is then amplitude-level encoded and then the DPSK signal is generated by symbol modulation with a carrier frequency f_c (i.e., $\sqrt{\frac{2}{T_b}}\cos(2\pi f_c t)$). The differential encoding starts with an arbitrary first bit or bit sequence (i.e., M-ary DPSK case) which serves as the reference. To be specific, the differential encoding is performed by modulo 2π addition. The input binary sequence has the absolute phase. Firstly, the absolute phase of the reference bit or bit sequence is compared with that of new input binary sequence. The phase difference of them means the differentially encoded phase sequence. The differentially encoded sequence is then determined by differentially encoded phase sequence.

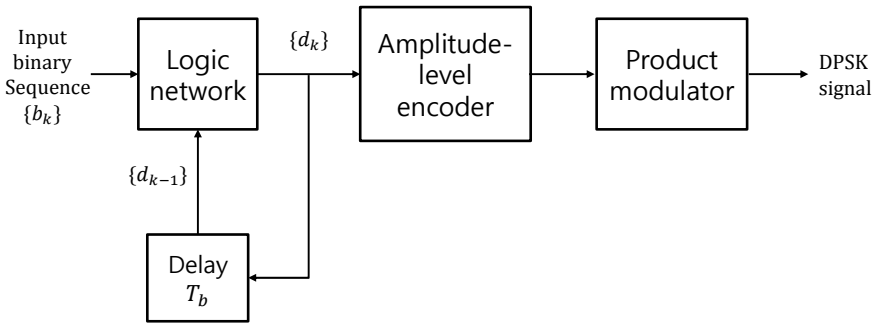

Figure 2.1 Block diagram for DPSK transmitter

The DPSK signals generated by above operations are transmitted to the receiver. The receiver detects the received DPSK signals. When this signal is detected, the receiver takes advantage of the fact that the phase-modulated pulses with two successive bits are equivalent except for a sign reversal. Thus the incoming pulse is multiplied by the preceding pulse, which actually means that the preceding pulse is used as the object of a locally generated reference signal. Figure 2.2 shows the receiver configuration for the detection of the DPSK signals; for the sample, integer $m = 0, \pm 1, \pm 2, ...$ Making a comparison between the DPSK detector of Figure 2.2 and the coherent PSK detector of Figure 2.3, we can see that the two receiver configurations are similar except for the locally generated reference signal.

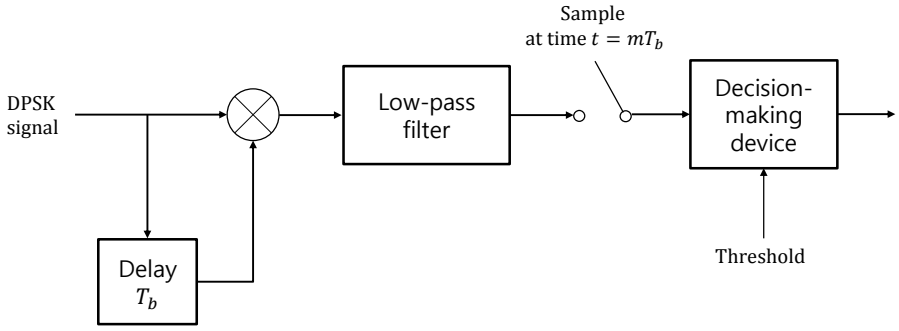

Figure 2.2 Block diagram for DPSK receiver

As previously mentioned, it can be noticed from Figure 2.2 that if the information of the first reference bit inserted at the first of the incoming binary data stream is given, the detection of DPSK signals can be achieved. In particular, if the sampled output of the low-pass filter applies to a decision-making device which has a fixed threshold, the detection of the DPSK signals is achieved. Here again, the receiver is assumed to be supplied with bit-timing information for the sampler to properly work.

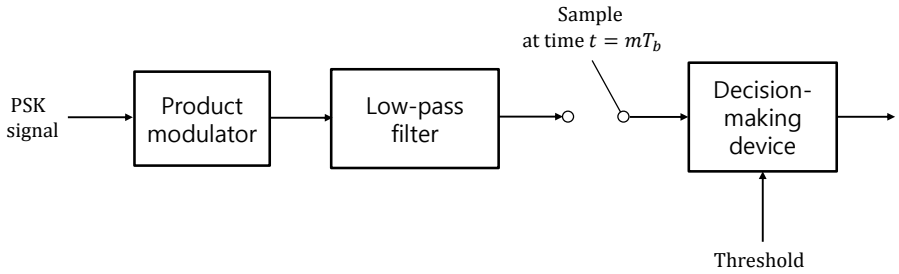

Figure 2.3 Block diagram for PSK receiver

In this paper, a non-coherent M-ary DPSK system is employed. Since a non-coherent system does not require synchronizing circuit for phase synchronization of a reference signal such as phase-locked loop, the system complexity is low, and thus the power consumption is lower than that of the coherent system. In this paper, we employ a non-coherent M-ary DPSK system because of these properties of them.

B. Repetition code

The repetition code is a well-known basic error-correcting code. To transmit a message over a noisy channel that may corrupt the transmitted signal, the concept of the repetition code is to just repeat the transmitted message multiple times. We hope that the channel corrupts only a minority of these repeated messages. The main attraction of the repetition code is that the implementation is very simple. However, some repetition codes might result in large trade-off between data rate and bit error rate (BER), and other types of error correcting codes can offer superior performance in these areas. The encoder and decoder of the repetition code in detail is provided in the following. The encoder is to repeat a particular bit multiple times to the waveform modulator when the bit is received from the bit source stream [25].

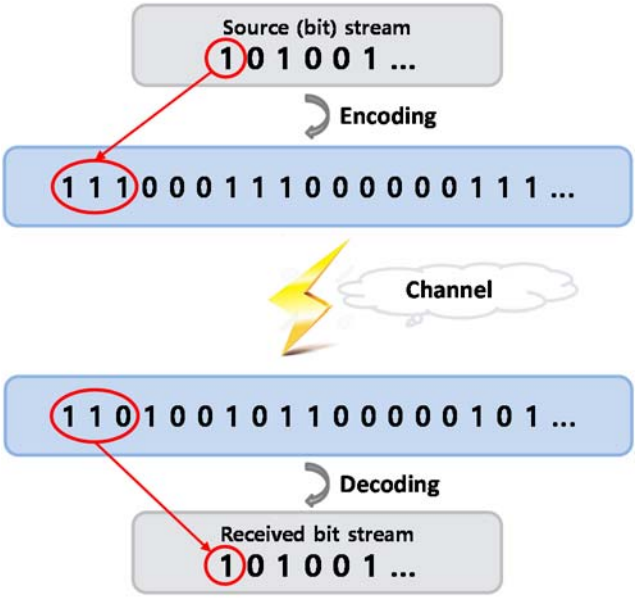

Figure 2.4 Encoder and Decoder of (3, 1) repetition code

For example, if we have a (3, 1) repetition code, then encoding the source stream *m=101001…* yields a code *c=111000111000000111…* as shown in Figure 2.4. The repetition decoding is usually done by majority logic detection [26]. In order to determine the value of a particular bit, we choose the value of a bit that occurs more frequently, looking at the copies of the bit in the received stream. For example, as depicted in Figure 2.4, the signal, which is received over the channel, *c=110100101100000101…* is decoded in accordance with majority logic detection and then the decoded message becomes *m=101001….* We will utilize the repetition property of repetition code for symbols in this research, which is named "symbol repetition" in this paper.

C. Previous researches

Our leading motive is to achieve low-power and reliable communications by using a non-coherent M-ary DPSK with symbol repetition. Unlike our research which employs symbol repetition, the IEEE 802.15.6 Wireless Body Area Network (WBAN) and IEEE P1901.2 employ M-ary DPSK modulation with bit spreader and interleaver for reliability improvement

[21] [22] [23]. They repeat an input bit sequence using a bit spreader with spreading factor of s=1, 2 or 4. For a spreading factor of s=2 and s=4, each input bit is repeated two times and four times as shown in Figure 2.5(a) and 2.5(b), respectively.

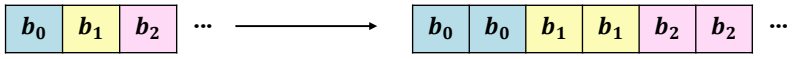

(a) Spreading factor = 2

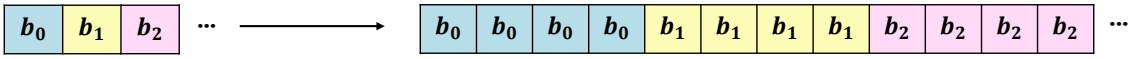

(b) Spreading factor = 4

Figure 2.5 Spreading scheme

After that, the output of the spreader shall be interleaved prior to modulation to provide robustness against error propagation. That is, high reliability can be achieved by interleaving spreaded bits. However, for DBPSK transmission, its performance is degraded when bit spreader and interleaver are applied, where the performance degradation clearly becomes larger as signal power reduces [27]. On the other hand, for DQPSK case, bit spreader and interleaver can cause performance improvement [27]. In this study, a symbol interleaver is not employed unlike previous researches, because it can be helpful in energy efficiency. This work demonstrates that the performance enhancement can be achieved without interleaving a symbol sequence, and the proposed scheme can achieve more performance improvement than the previous researches.

III. SYSTEM MODEL

A. Symbol repetition model

In this work, a non-coherent DPSK modulation and a repetition scheme is assumed as the system model, where the overall system model is illustrated in Figure 3.1. To be specific, DPSK pre-symbol d_k at the *k*-th symbol time is expressed as

$$d_k = s_k s^*_{k-1}. \tag{3.1}$$

Thus, a DPSK symbol s_k is denoted by

$$s_k = d_k s_{k-1}. \tag{3.2}$$

We consider only the assumption that no symbol interleaver is employed and thus the *k*-th pre-symbol d_k and (*k*+1)-th pre-symbol d_{k+1} have the same information. Also, the channel is regarded as the additive white Gaussian noise (AWGN) channel. Finally, in receiver, symbol reconstruction is performed by the inverse of symbol transmission in transmitter.

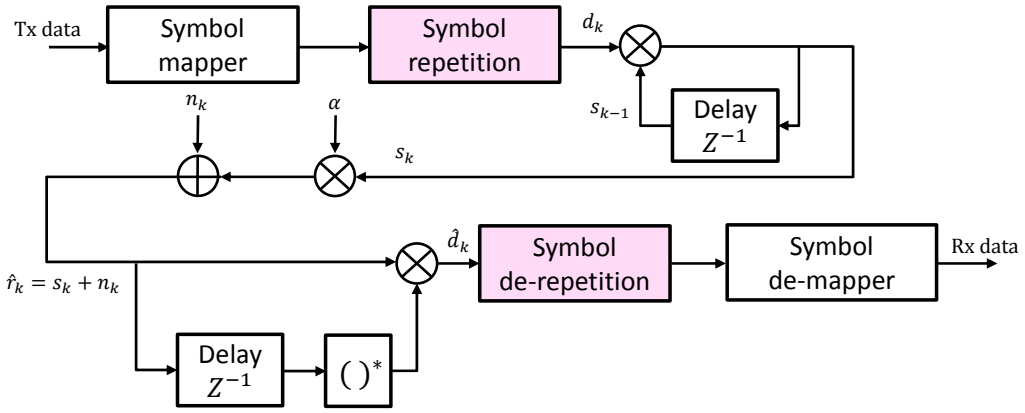

Figure 3.1 System block diagram

The specific transmission and detection procedures are as follows. The DPSK transmission system with symbol repetition scheme generates pre-symbol $\{d_k\}$ by the grouping of $\log_2 M$ bits, where *M* is a modulation order. Then, the pre-symbol $\{d_k\}$ is repeated as *R* times, where

R is the repetition order. As mentioned above, it is assumed that the repeated pre-symbols are continuously ordered for performance improvement. After that, the pre-symbols are differentially encoded into DPSK symbols transmitted over the AWGN channel, and then the noisy DPSK symbol $\hat{r}_k$ at the k-th symbol time is expressed by

$$\hat{r}_k = \alpha s_k + n_k, \tag{3.3}$$

where $\alpha = \sqrt{E_b R^{-1} \log_2 M}$ is the signal gain and n_k is the k-th noise term. The noisy DPSK symbols are differentially decoded, and the decoded pre-symbol $\hat{d}_k$ can be expressed as

$$\begin{aligned} \hat{d}_k &= \hat{r}_k \hat{r}^*_{k-1} \alpha^{-2} \\ &= \left(\alpha s_k + n_k\right)\left(\alpha s_{k-1} + n_{k-1}\right)^* \alpha^{-2} \\ &= s_k s^*_{k-1} + \left(s_k n^*_{k-1} + s^*_{k-1} n_k\right)\alpha^{-1} + n_k n^*_{k-1}\alpha^{-2} \\ &= d_k + \left(s_k n^*_{k-1} + s^*_{k-1} n_k\right)\alpha^{-1} + n_k n^*_{k-1}\alpha^{-2}. \end{aligned} \tag{3.4}$$

Then, the de-repetition of the pre-symbols is performed by

$$\hat{d}_{k,sum} = \frac{1}{R}\sum_{i=0}^{R-1} \hat{d}_{k,i}. \tag{3.5}$$

The decoded pre-symbol $\hat{d}_{k,i}$ of (3.5) contains the same information from $\hat{d}_{k,0}$ to $\hat{d}_{k,R-1}$. In the case of $R=2$, for example, the de-repetition of repeated decoded pre-symbols is performed by (3.5) as follow

$$\begin{aligned} \hat{d}_{k,sum} &= \frac{\hat{d}_k + \hat{d}_{k+1}}{2} = \frac{1}{2}\left[\left(\hat{r}_k \hat{r}^*_{k-1}\right) + \left(\hat{r}_{k+1}\hat{r}^*_k\right)\right]\alpha^{-2} \\ &= \frac{d_k + d_{k+1}}{2} + \frac{1}{2}\omega_k \\ &= d_k + \frac{1}{2}\omega_k. \end{aligned} \tag{3.6}$$

Since the *k*-th pre-symbol d_k and (*k*+1)-th pre-symbol d_{k+1} have the same information due to symbol repetition, $\frac{d_k + d_{k+1}}{2}$ of the second term in (3.6) can be expressed by d_k, where the pre-symbol d_k is desired signal. The noise term ω_k is obtained by expanding (3.6)

$$\begin{aligned}
\omega_k &= \left(s_k n^*_{k-1} + s^*_{k-1} n_k + s_{k+1} n^*_k + s^*_k n_{k+1}\right)\alpha^{-1} \\
&\quad + \left(n_k n^*_{k-1} + n_{k+1} n^*_k\right)\alpha^{-2} \\
&= \left(s_k n^*_{k-1} + d_k s^*_k n_k + d_k s_k n^*_k + s^*_k n_{k+1}\right)\alpha^{-1} \\
&\quad + \left(n_k n^*_{k-1} + n_{k+1} n^*_k\right)\alpha^{-2} \\
&= 2 d_k Re\left(s^*_k n_k\right)\alpha^{-1} + \left(s_k n^*_{k-1} + s^*_k n_{k+1}\right)\alpha^{-1} \\
&\quad + \left(n_k n^*_{k-1} + n_{k+1} n^*_k\right)\alpha^{-2}.
\end{aligned} \tag{3.7}$$

The $2\,\mathrm{Re}(s^*_k n_k)$ is obtained by a Hermitian quadratic form of complex variables [28] whose theorem is

$$z_k \triangleq 2\,\mathrm{Re}(u^*_k w_k) = u^*_k w_k + u_k w^*_k.$$

Interestingly, we observed that the decoding procedure of repeated symbol sequence results in the skewness for the distribution of the decoded signal. That is, the noise distribution may affect the distribution of a decoded pre-symbol, which causes variation in error rate. In addition, it can be also noticed that the intensity of skewness for ω_k varies due to *R*. The detailed explanation will be provided in Section Ⅳ.

IV. PERFORMANCE ANALYSIS

As mentioned earlier, the noise distribution is skewed by decoding criteria for repeated symbol sequence. To be specific, the shape of noise distribution affected by the skewness of ω_k may reduce or increase an error rate. In the case that a non-coherent DPSK system is used with symbol repetition, the decoded pre-symbol $\hat{d}_k$ contains the correlated noise. Thus, the noise included in the decoded pre-symbol $\hat{d}_k$ is skewed. To discuss this phenomenon, we consider a constellation diagram in Figure 4.1, which is the constellation diagram of D8PSK. When the transmitted signal constellation point is given, the received signal points that are not located within the successful detection area in Figure 4.1 are regarded as error. If the noise distribution of the decoded pre-symbol $\hat{d}_k$ is well fitted to an error decision boundary, the signal point of decoded pre-symbols is located more within the successful detection area. That is, it means that the symbol error rate (SER) becomes low even the received SNR is identical. The important fact is that the SER depends on the power of noise as well as the noise distribution shape. We analyze an influence of the skewness for an error rate and examine the effect of noise distribution shape by the skewness in next Subsection 4.1 and 4.2.

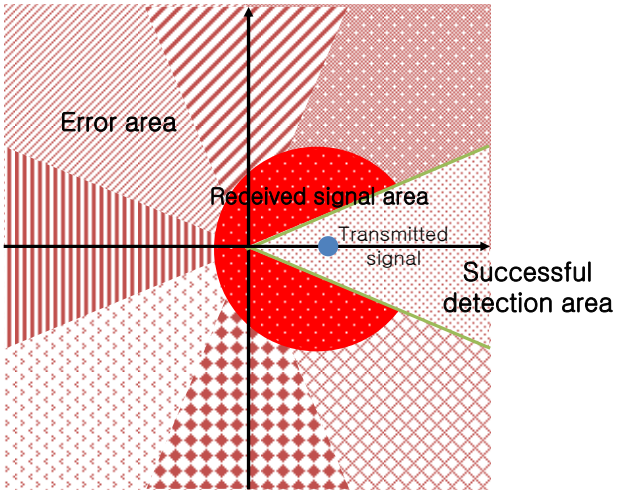

Figure 4.1 D8PSK constellation diagram

A. Skewness approach

In this Subsection, we examine a derivation of the noise distribution shape by the skewness of ω_k in (3.7). The *R=2* scenario is considered for better understanding, where the overall tendency of the analysis can be preserved without loss of generality. For analysis, define n'_{k-1} and n'_{k+1} as

$$n'_{k-1} = \frac{n^*_{k-1}(s_k + \alpha^{-1}n_k)}{\left|s_k + \alpha^{-1}n_k\right|},\ n'_{k+1} = \frac{n_{k+1}(s_k + \alpha^{-1}n_k)^*}{\left|s_k + \alpha^{-1}n_k\right|}.$$

Then, we can rearrange ω_k in (3.7) as

$$\begin{aligned}\omega_k &= \frac{2d_k\,\mathrm{Re}(s^*_k n_k) + s_k n^*_{k-1} + s^*_k n_{k+1}}{\alpha} + \frac{n_k n^*_{k-1} + n_{k+1}n^*_k}{\alpha^2} \\ &= \frac{2d_k\,\mathrm{Re}(s^*_k n_k) + (s_k + \alpha^{-1}n_k)n^*_{k-1} + (s^*_k + \alpha^{-1}n^*_k)n_{k+1}}{\alpha} \\ &= \frac{2d_k\,\mathrm{Re}(s^*_k n_k)}{\alpha} + \frac{\left|\alpha s_k + n_k\right|}{\alpha^2}(n'_{k-1} + n'_{k+1}) \\ &= \frac{2d_k\,\mathrm{Re}(s^*_k n_k)}{\alpha} + \frac{\sqrt{\alpha^2 + 2\alpha\,\mathrm{Re}(s^*_k n_k) + \left|n_k\right|^2}}{\alpha^2}(n'_{k-1} + n'_{k+1}).\end{aligned} \tag{4.1}$$

Due to the dependence resulting from $\mathrm{Re}(s^*_k n_k)$, the intuitive understanding of the noise distribution shape is still difficult. Thus, this is discussed in two phases. In the first phase, s_k and n_k are assumed to be 'static' value and 'given'. As showed above, we can know the correlation coefficient between $\mathrm{Re}(s^*_k n_k)$ and $\left|\alpha s_k + n_k\right|$ is positive, since

$$\left|\alpha s_k + n_k\right| = \sqrt{\alpha^2 + 2\alpha\,\mathrm{Re}(s^*_k n_k) + \left|n_k\right|^2}.$$

Note that the phase of $(n'_{k-1} + n'_{k+1})$ is uniformly distributed on $(0, 2\pi]$. Thus, when $\mathrm{Re}(s^*_k n_k)$ is large, $\left|\alpha s_k + n_k\right|$ also has a large value, and consequently it causes a high power Gaussian noise of mean $2d_k\,\mathrm{Re}(s^*_k n_k)\alpha^{-1}$. when $\mathrm{Re}(s^*_k n_k)$ is low, low power noise has

mean value $2d_k \mathrm{Re}(s^*_k n_k)\alpha^{-1}$. Now let s_k and n_k be random variables. Even if $\mathrm{Re}(s^*_k n_k)$ is also a random variable, previously introduced properties remain. As a result, the noise distribution shape of ω_k results from overlaps of uniform phase noises with different $\mathrm{Re}(s^*_k n_k)$ values as shown in Figure 4.2.

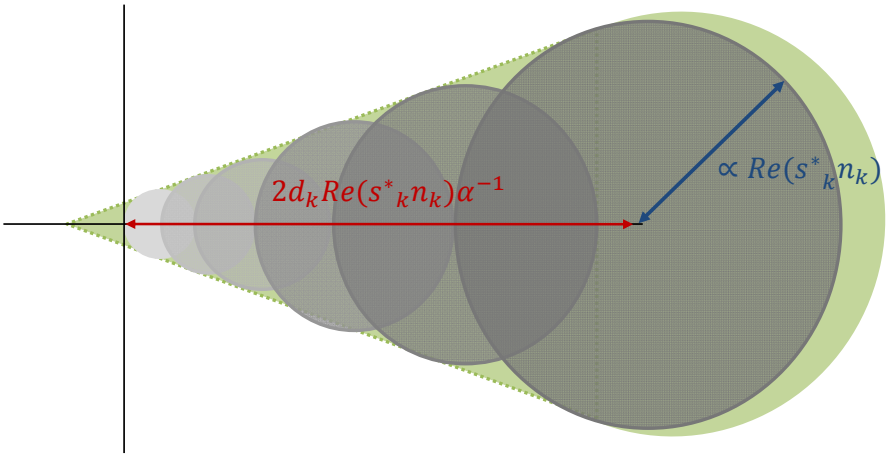

Figure 4.2 Analysis of noise distribution shape

B. Effect of noise distribution shape

The previous Subsection discussed the decoded symbol distribution affected by the skewness of ω_k. Next, the error rate of de-repeated pre-symbols will be provided. For fair comparison, it is conducted under an identical SNR condition. Firstly, DQPSK cases are introduced as shown in Figure 4.3 and 4.4. In Figure 4.3, the more skewed one is received signal points of DQPSK system with repetition and the other is de-repeated signal points of DQPSK system without repetition. The dotted line is the error decision boundary, which decides whether it is an error or not. The signal point located in left side of the error decision boundary is an error. Since the received signal point of DQPSK with non-repetition is located more outside the error decision boundary, it is clear that the error of DQPSK with repetition is lower.

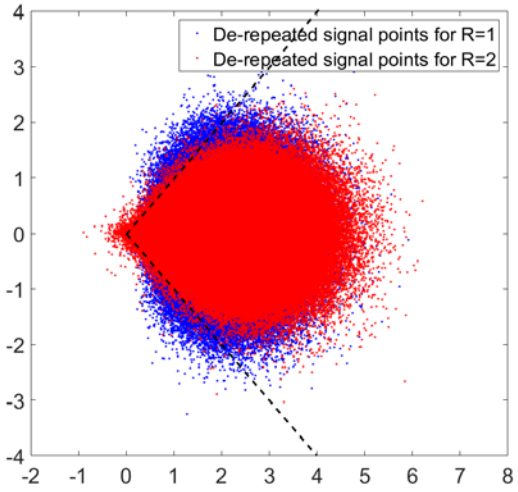

Figure 4.3 Comparison of received signal constellation point for DQPSK case

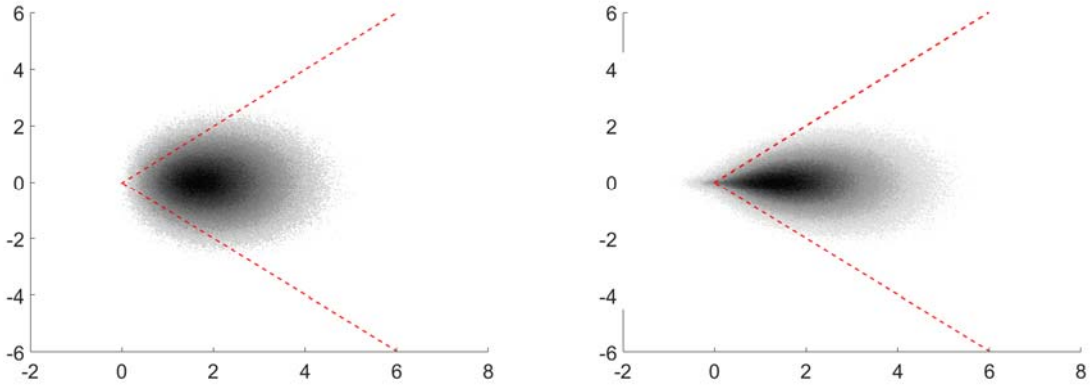

(a) DQPSK without repetition (b) DQPSK with repetition for R=2

Figure 4.4 Error rate comparison for DQPSK case

Figure 4.4(a) and 4.4(b) are the distribution of a de-repeated DQPSK pre-symbol without repetition and with repetition, respectively. The distribution of them results from the noise distribution shape. In Figure 4.4, the dotted line is the error decision boundary. The distribution of a de-repeated DQPSK pre-symbol without repetition shows the near-Gaussian form. On the other hand, the distribution of a de-repeated DQPSK pre-symbol with repetition is skewed. Thus one can recognize that the distribution of the de-repeated DQPSK pre-symbol with repetition fits better to the error decision boundary than that of the de-repeated DQPSK pre-

symbol without repetition, as shown in Figure 4.4. This means that the distribution shape of DQPSK with repetition may change the error rate significantly. In the case of Figure 4.4, the error rate of DQPSK with repetition is lower than that of DQPSK without repetition. Note that the noise distribution of M-ary DPSK with our proposed scheme can reduce or increase an error rate according to relations between M and R. Thus, we should choose the proper R in accordance with M so as to obtain performance gain. The more R is, the noise distribution of DQPSK with repetition increasingly becomes the Gaussian form by the central limit theorem.

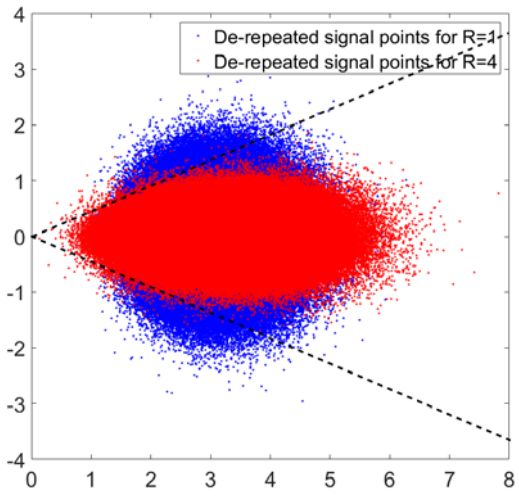

Figure 4.5 Comparison of received signal constellation point for D8PSK case

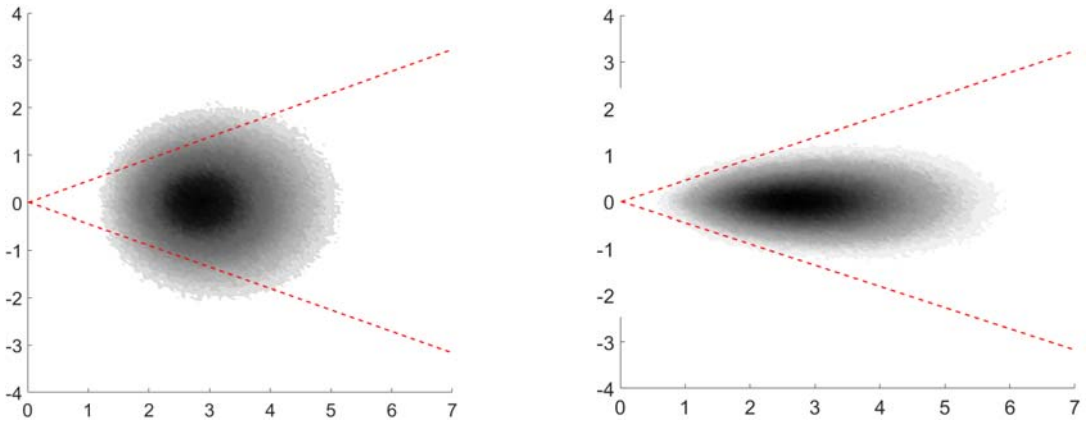

(a) D8PSK without repetition (b) D8PSK with repetition for R=4

Figure 4.6 Error rate comparison for D8PSK case

Similarly, for $M \geq 8$, we can achieve the identical effect to DQPSK case by using our proposed scheme. This is verified via Figure 4.5 and 4.6 (i.e., D8PSK case).

C. Further performance enhancement

Note that there is information on a decoded pre-symbol $\hat{d}_k$ unused in de-repetition process for our proposed scheme. In fact, further performance improvement can be achieved by exploiting unused information as the special case model of our proposed scheme. At the cost of marginal complexity increment due to the additional decoding operation, we expect that the effect of performance improvement is much more significant because of the simplicity of decoding operation.

3.1 Method for further performance improvement

The special case model is subject to the symbol repetition model. As mentioned above, a non-coherent M-ary DPSK with symbol repetition scheme still remains further information available on a decoded pre-symbol $\hat{d}_k$ for the de-repetition. In other words, it can be additionally used for the symbol reconstruction, and further improvement in detection performance can be achieved for certain *M* and *R* scenarios. If *M* and *R* have the certain relations, noisy pre-symbols prior to decoding are located in separate phase. For example, in the case of *M=4* and *R=3*, noisy pre-symbols are received to one of four phases on $(0, \frac{\pi}{2}, \pi, \frac{3\pi}{2})$ and each of them lies at four separate phases. This property may be satisfied with the case that *M* and *R* are the relative prime. For better understanding, we examine further information on a decoded pre-symbol $\hat{d}_k$ through Figure 4.7 for DQPSK and D8PSK cases.

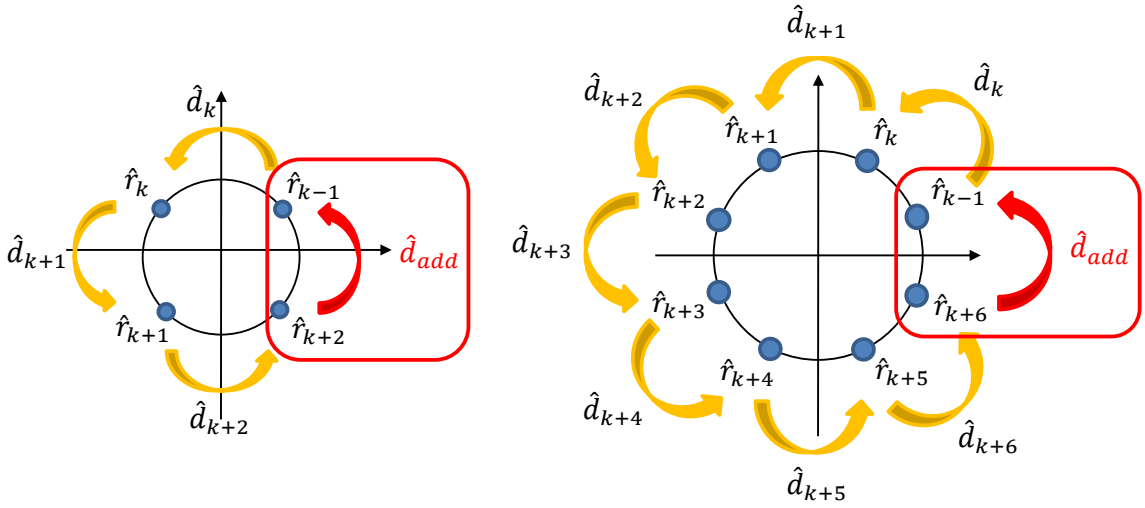

(a) Further information for DQPSK case (b) Further information for D8PSK case

Figure 4.7 Anaylsis of unused further information

As shown in Figure 4.7(a), in the case of *M=4* and *R=3*, we can utilize further information $\hat{d}_{add}$ for the symbol reconstruction. Note that $\hat{d}_k$, $\hat{d}_{k+1}$ and $\hat{d}_{k+2}$ include the same information, because *R=3*. Interestingly, further information $\hat{d}_{add}$ also contains the same information with them. The same applies to Figure 4.7(b) of the case of *M=8* and *R=7*. By further information $\hat{d}_{add}$, the de-repetition process of (3.5) is modified into

$$\hat{d}_{k,sum} = \frac{1}{R}\sum_{i=0}^{R-1}\hat{d}_{k,i} + \hat{d}_{add}. \tag{4.2}$$

As a result, the receiver can reconstruct the *k*-th pre-symbol via (4.2) and consequently higher reliability than symbol repetition model can be obtained with marginal complexity increment.

3.2 Performance analysis for special case model

By further information, the skewness of ω_k more strongly affects a noise distribution shape in the special case model than in the symbol repetition model. For certain *M* and *R* scenario,

we compare the error rate of a de-repeated pre-symbol between the symbol repetition model and the special case model in the same way as Section 4.2.

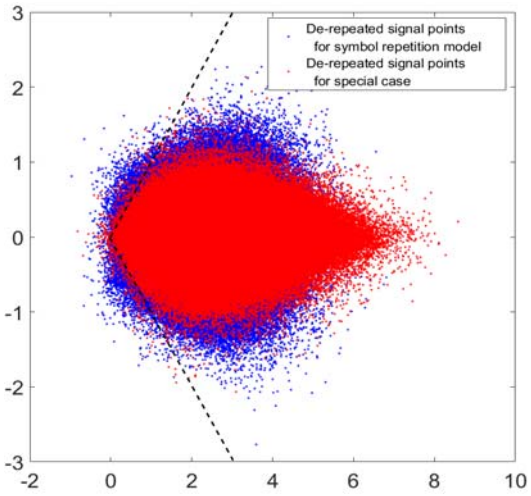

Figure 4.8 Comparison of received signal constellation point for DQPSK case

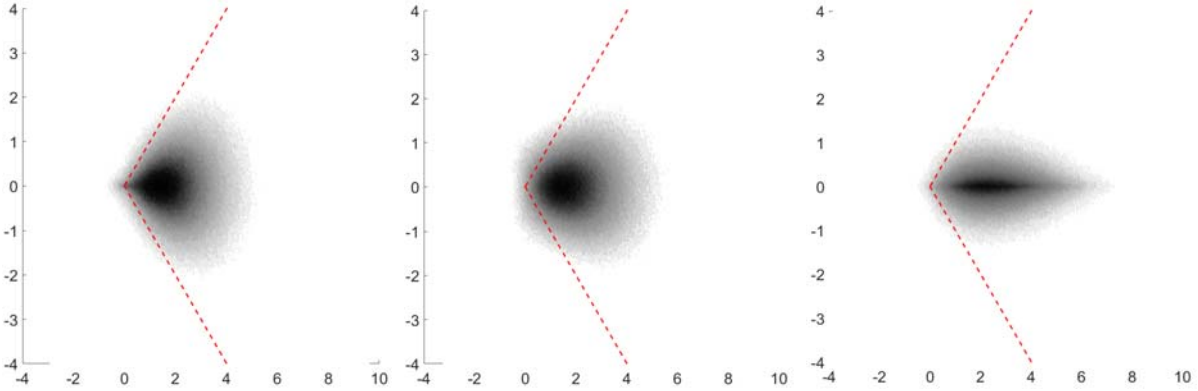

(a) For *R=2* (Symbol repetition model)

(b) For *R=3* (Symbol repetition model)

(c) For *R=3* (Special case model)

Figure 4.9 Error rate comparison for DQPSK case

Figure 4.8 shows comparison of signal constellation point of de-repeated pre-symbols for both cases. The more skewed one is de-repeated signal points for the special case model and the other is de-repeated signal points for the symbol repetition model. This was performed for *M=4* and *R=3* scenario. We can know that the special case model which includes further information may generate lower error than the symbol repetition model. Figure 4.9 shows the distribution

shape of de-repeated pre-symbols for 3 cases. Figure 4.9(a) and 4.9(b) are the symbol repetition model and Figure 4.9(c) is the special case model. For fair comparison, it was compared under identical SNR condition. For the same *R*, we can confirm that the error rate of special case is lower than that of symbol repetition model by comparing Figure 4.9(b) and 4.9(c). The error performance for special case model of Figure 4.9(c) is even better than that for symbol repetition model of Figure 4.9(a) which has the best error performance. Even if the system complexity increases by additional decoding operation, in some application where power is at a premium (e.g., in digital satellite communications) even a 1dB saving in SNR is well worth the effort.

In next Section Ⅴ, we prepared the simulation and experimental results for performance evaluation.

V. SIMULATION AND EXPERIMENT RESULTS

In this Section, the performance of a non-coherent M-ary DPSK receiver with symbol repetition is evaluated. In addition, performance evaluation for special case model is additionally considered. The simulation results are also provided to show the performance of a non-coherent M-ary DPSK with symbol repetition by comparing them with experimental results. In addition, the experiment was performed to evaluate performance in a real channel environment.

Figure 5.1 Software defined radio USRP N210

As shown in Figure 5.1, the proposed system is implemented by using the software defined radio (SDR) USRP N210 for real-world performance evaluation [29]. The SDR USRP N210 has various functions such as recording and generation of an RF signal. It can also interact with a computer for the transmission and reception of a signal, and be controlled by support software that allows users to easily deal with any process such as numerical calculus of data. In this experiment, MATLAB was used for simple implementation, and the sampling rate and symbol rate were set at 195 kHz and 48 kHz, respectively. Figure 5.2 shows the schematic diagram for the experimental setting. A pseudo-noise generator generates a noise, and then an air channel is corrupted by the noise. The transmitter and receiver are connected over the wireless channel.

Under such setting, the bit error rate (BER) performance of the implemented system is measured for various transmit power of the pseudo-noise generator.

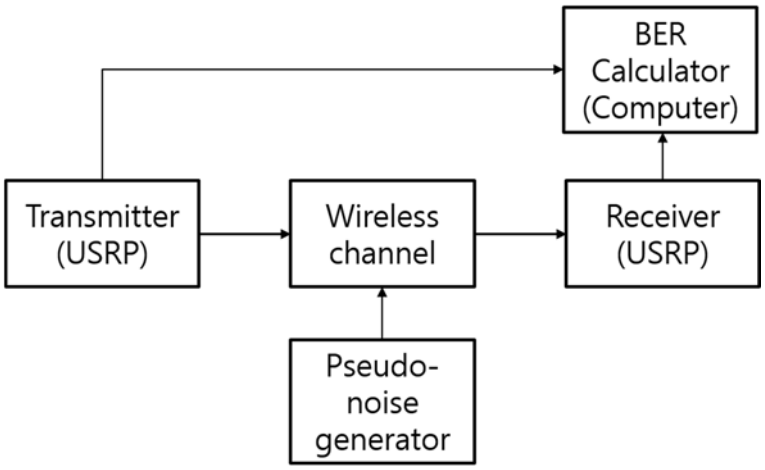

Figure 5.2 Schematic diagram for experimental setting

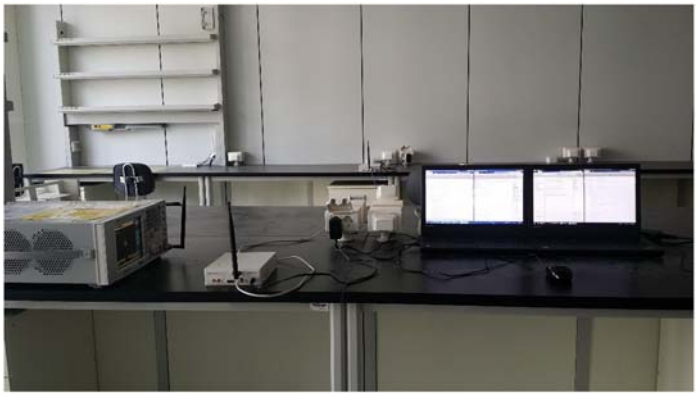

(a) Real experimental setting

(b) N5182A MXG Signal Generator (c) N9030A PXA Signal Analyzer

Figure 5.3 Real configuration for experimental setting

The real-world configuration for experimental setting is shown in Figure 5.3. For experiment, the N5182A MXG signal generator of Figure 5.3(b) and N9030A PXA signal analyzer of Figure 5.3(c) were used [30] [31]. Figure 5.3(a) is the real experimental setting. Figure 5.8, 5.9, and 5.10 of Section 5.2 show BER performance curves of a non-coherent M-ary DPSK with symbol repetition for the special case model that additionally uses information which is not utilized in de-repetition process of the symbol repetition model for the symbol reconstruction. The BER performance on the special case model will be evaluated by comparing it with the BER performance on the symbol repetition model, since the special case model is subject to the symbol repetition model.

A. Performance evaluation of symbol repetition model

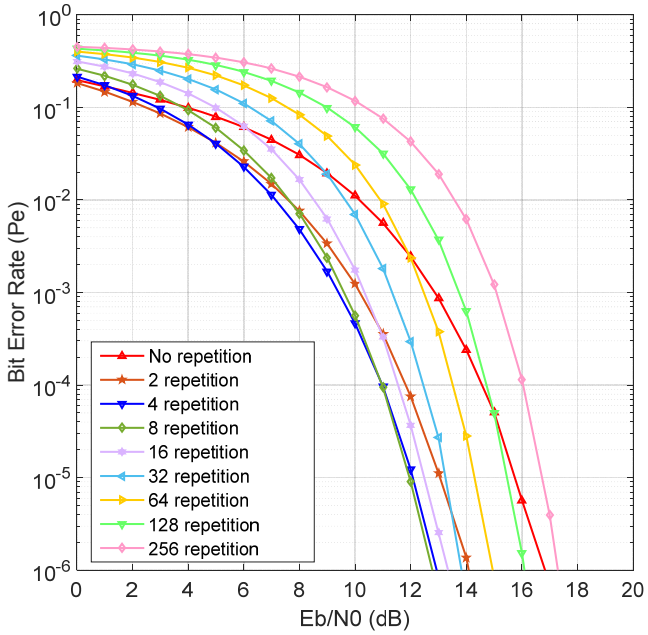

Figure 5.4 BER curves for D8PSK case

Firstly, the BER performance of a non-coherent M-ary DPSK with the proposed scheme is simulated. Figure 5.4 shows the BER performance of D8PSK with symbol repetition. As shown

in Figure 5.4, the application of the symbol repetition model for D8PSK system can obtain the effect of performance improvement. For *R=4* case, the BER performance of D8PSK system with symbol repetition shows the lowest BER throughout all repetition orders. Its performance is about 4dB better than D8PSK without repetition in $P_e \leq 10^{-4}$. The BER performance of D8PSK system with symbol repetition, in common with DQPSK repetition system, begins to get worse from a certain *R*. Therefore, we should choose a proper *R* considering requirements of a desired application, and employ M-ary DPSK system with symbol repetition only in the case that an application requires low data rate.

Repetition order (*R*)	BER in PN noise power [17 dBm]
1 (No rep.)	0.0876
2	0.0109
4	**0.0042**
8	0.0058
16	0.0299
32	0.0385
64	0.0959
128	0.1324
256	0.2176

TABLE 5.1 BER measurement results for D8PSK case

TABLE 5.1 shows BER measurement results for D8PSK in a real environment. Because there are non-ideal experimental errors such as symbol-timing error and frequency offset, experimental results do not accurately match to simulation results. However, the tendency of experiment results perfectly matches with that of simulation results. As shown in Figure 5.5, the tendency of BER performance curves for D16PSK system with symbol repetition is also similar to D8PSK. In the case of $R = 8$, the BER performance of D16PSK system with symbol repetition is about 6dB better than that of D16PSK system without repetition for $P_e \leq 10^{-4}$ and the best throughout all repetition orders. If a communication system which

employs D16PSK modulation requires high reliability, the proposed scheme can be applied to the system so as to obtain higher reliability. Since the tendency of experiment result in TABLE 5.2 is identical with that of simulation result of Figure 5.5, our proposed scheme is sufficiently trustworthy.

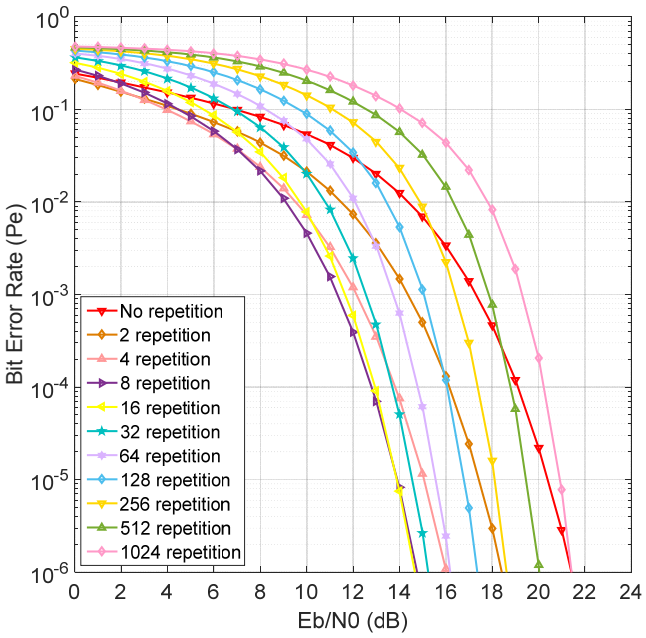

Figure 5.5 BER curves for D16PSK case

Repetition order (R)	BER in PN noise power [10 dBm]
1 (No rep.)	0.0278
2	0.0115
4	0.0101
8	**0.008**
16	0.0092
32	0.0109
64	0.0245
128	0.0673
256	0.1052
512	0.2132

TABLE 5.2 BER measurement results for D16PSK case

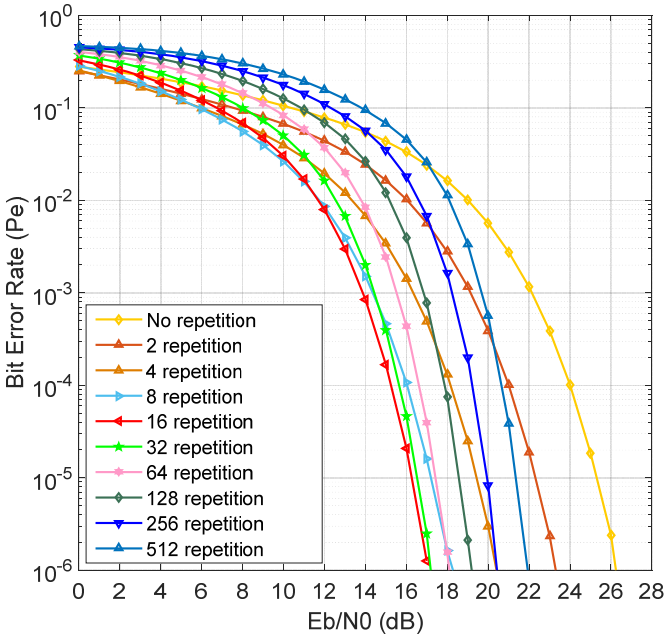

Figure 5.6 BER curves for D32PSK case

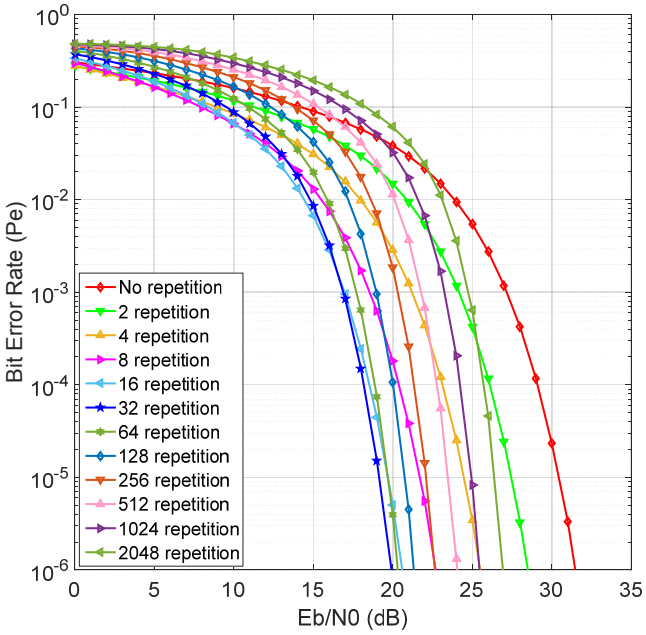

Figure 5.7 BER curves for D64PSK case

D32PSK and D64PSK systems with symbol repetition have the best performance at $R = 16$ and $R = 32$, respectively. In addition, one can find that performance enhancement of about

9dB and 11dB gain in E_b/N_0 is achieved for $P_e \leq 10^{-4}$ from Figure 5.6 and 5.7. Since the fact that match between the tendency of simulation and experimental result is already verified, an experiment for D32PSK or $M \geq 32$ cases was not performed in this study. As a result, one can notice that a non-coherent M-ary DPSK system with the proposed scheme can achieve the best BER performance, when *R* is a half of *M*. That is, from the numerical results, the *R* for the best BER performance in the symbol repetition model can be defined as

$$R = \frac{M}{2}.$$

B. Performance evaluation of special case model

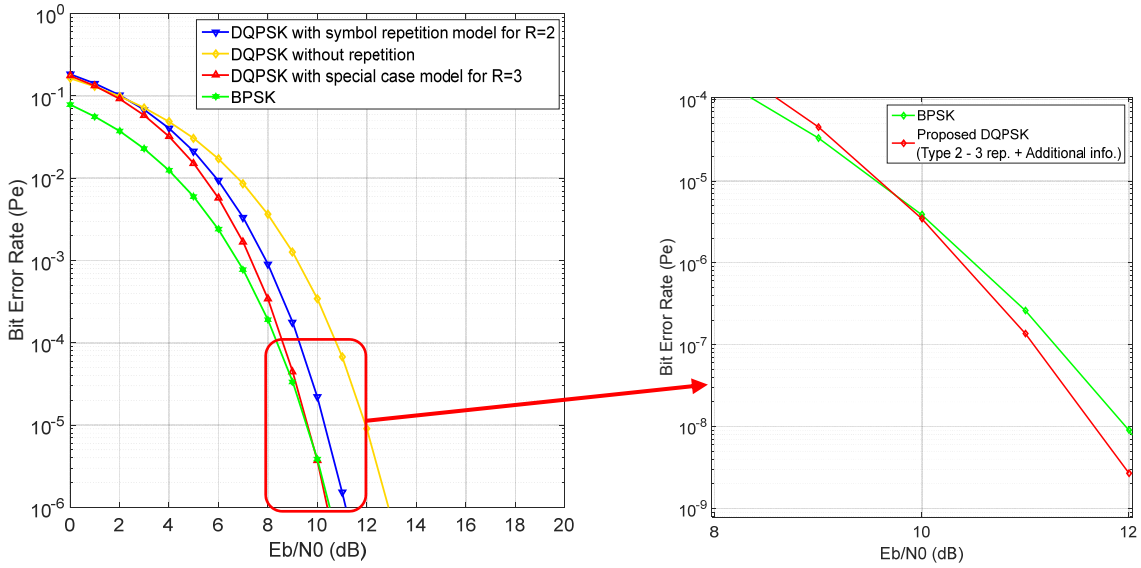

Figure 5.8 BER curves for DQPSK case

Note that the special case model is subject to the symbol repetition model, meaning that the BER performance for the symbol repetition model is best at the special case model. Thus, it can be concluded that further information obtained by the special case model positively influences the system performance. In Figure 5.8, the BER performance of DQPSK system

with the special case model is compared with the BER performance of DQPSK system with the symbol repetition model, DQPSK system without repetition, and BPSK. For instance, the BER performance of DQPSK system with repetition is better than that of DQPSK system without repetition (see Figure 5.8). The upward-pointing triangle line and downward-pointing triangle line of Figure 5.8 mean the BER performance curve for the special case model and the symbol repetition model, respectively. In order to compare only the BER performance between the symbol repetition model and the special case model, we considered the *R* only which makes it to have the best BER performance for each model. As shown in Figure 4.9 of Subsection 4.3.2, we can know that the BER performance of DQPSK system with the special case model is the best of them. Interestingly, in the case of $M = 4,$ its BER performance gets better than that of BPSK for $P_e < 10^{-5}.$ Even though the complexity might increase with *M*, the increment is quite marginal and the BER performance beyond BPSK may be significantly helpful in some applications. When the special case model is applied to M-ary DPSK system for $M \geq 4,$ proper choice of *R* is necessary with consideration for a trade-off between complexity and performance according to application requirements. Figure 5.9 and 5.10 are BER curves for D8PSK and D16PSK case, respectively. D8PSK case of Figure 5.9 is for $M = 8$ and $R = 7$ scenario, and D16PSK case of Figure 5.10 is for $M = 16$ and $R = 15$ scenario. Through these results, the *R* for the best BER performance in the special case model can be expressed as

$$R = M - 1.$$

Finally, when the special case model is applied, higher reliability than the symbol repetition model can be obtained with marginal complexity increment. Therefore, once again, a proper *R* should be adopted considering application requirements.

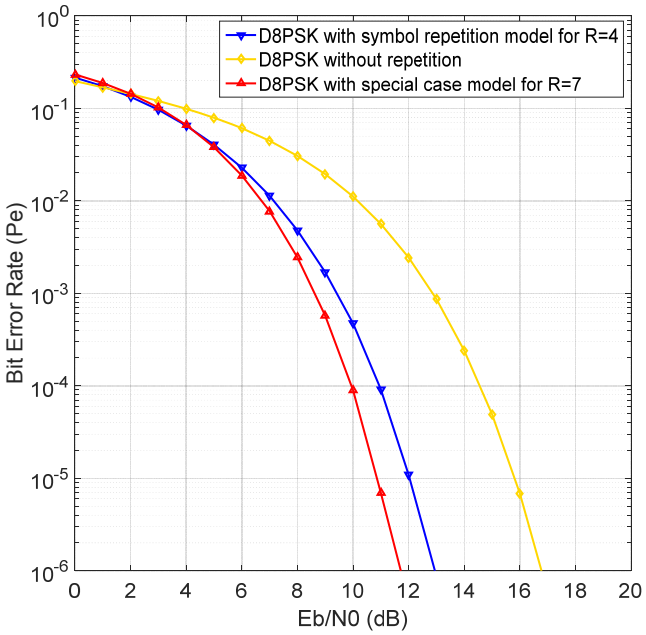

Figure 5.9 BER curves for D8PSK case

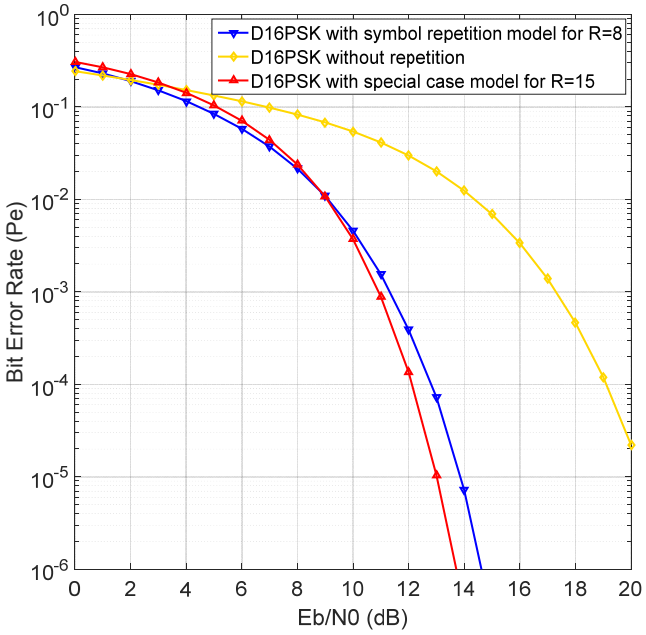

Figure 5.10 BER curves for D16PSK case

VI. CONCLUSION

In this paper, the performance of a non-coherent M-ary DPSK receiver with symbol repetition is analyzed for low-power and reliable communications. The analysis and numerical performance evaluation show that this scheme is able to improve the energy efficiency as well as the communication reliability in all modulation order, except for DBPSK. The performance of a non-coherent M-ary DPSK with symbol repetition varies according to the modulation order and repetition order. To be specific, the distribution of a received signal influenced by noise characteristic is observed to be skewed, and if this distribution is well fitted to an error decision boundary, its demodulator achieves lower error rate and vice versa. Furthermore, we achieve performance improvement by additionally decoding unused information at the cost of system complexity. We expect that our proposed scheme is helpful in a variety of communication systems (e.g., IEEE 802.15.6 WBAN and IEEE P1901.2) for low-power and reliable communication systems due to design simplicity and better performance.

REFERENCE

[1] Lin, T. H., William J. K., and Gregory J. P. "Integrated low-power communication system design for wireless sensor networks." *IEEE Communications Magazine*, 42(12), 2004, pp. 142-150.

[2] Heinzelman, W. R., Chandrakasan, A., and Balakrishnan, H. "Energy-efficient communication protocol for wireless microsensor networks." *System sciences, 2000. Proceedings of the 33rd annual Hawaii international conference on.* IEEE, 2, 2000, pp. 10-pp.

[3] Bradley, P. D. "An ultra low power, high performance medical implant communication system (MICS) transceiver for implantable devices." *2006 IEEE Biomedical Circuits and Systems Conference*. IEEE, 2006, pp. 158-161.

[4] G. M. Strohallen et al. "*Low power wireless communication system employing magnetic control zones*", US Patent 5, 774, 791, Patent and Trademark Office, 1998.

[5] Schurgers, C., Aberthorne, O., and Srivastava, M. "Modulation scaling for energy aware communication systems." *Proceedings of the 2001 international symposium on Low power electronics and design*, ACM, 2001, pp. 96-99.

[6] Atzori, L., Iera, A., and Morabito, G. "The internet of things: A survey." *Computer networks.* 54(15), 2010, pp. 2787-2805.

[7] Gubbi, J., Buyya, R., Marusic, S., and Palaniswami, M. "Internet of Things (IoT): A vision, architectural elements, and future directions." *Future Generation Computer Systems*, 29(7), 2013, pp. 1645-1660.

[8] Da Xu, L., He, W., and Li, S. "Internet of things in industries: A survey." *IEEE Transactions on Industrial Informatics,* 10(4), 2014, pp. 2233-2243.

[9] Columbus, L. *Roundup Of Internet of Things Forecasts And Market Estimates, 2015*, 2016.

[10] Sheng, Z., Mahapatra, C., Zhu, C., and Leung, V. C. "Recent advances in industrial wireless sensor networks toward efficient management in IoT." *IEEE Access,* 3, 2015, pp. 622-637.

[11] Heragu, A., Ruffieux, D., and Enz, C. *The design of ultralow-power MEMS-based radio for WSN and WBAN*, Frequency References, Power Management for SoC, and Smart Wireless Interfaces, Springer International Publishing, 2014. 265-280 pages.

[12] Yick, J., Mukherjee, B., and Ghosal, D. "Wireless sensor network survey." *Computer networks*, 52(12), 2008, pp. 2292-2330.

[13] Enz, C., Scolari, N., and Yodprasit, U. "Ultra low-power radio design for wireless sensor networks." *2005 IEEE International Wkshp on Radio-Frequency Integration Technology: Integrated Circuits for Wideband Comm & Wireless Sensor Networks*, IEEE, 2005, pp. 1-17.

[14] Daly, D. C., and Chandrakasan, A. P. "An energy-efficient OOK transceiver for wireless sensor networks." *IEEE Journal of Solid-State Circuits*, 42(5), 2007, pp. 1003-1011.

[15] Lee, J., Chen, Y., and Huang, Y. "A low-power low-cost fully-integrated 60-GHz transceiver system with OOK modulation and on-board antenna assembly." *IEEE Journal of Solid-State Circuits*, 45(2), 2010, pp. 264-275.

[16] Bae, J., and Yoo, H. J. "A 45 W Injection-Locked FSK Wake-Up Receiver With Frequency-to-Envelope Conversion for Crystal-Less Wireless Body Area Network." *IEEE Journal of Solid-State Circuits*, 50(6), 2015, pp. 1351-1360.

[17] Bae, J., Yan, L., and Yoo, H. J. "A low energy injection-locked FSK transceiver with frequency-to-amplitude conversion for body sensor applications." *IEEE Journal of Solid-state circuits*, 46(4), 2011, pp. 928-937.

[18] Bae, J., Cho, N., & Yoo, H. J. "A 490uW fully MICS compatible FSK transceiver for implantable devices." *2009 Symposium on VLSI Circuits*, IEEE, 2009, pp. 36-37.

[19] Haykin, S. S., Moher, M., and Song, T. *An introduction to Analog and Digital Communications*, Wiley, NewYork, 2006, 293-295 pages.

[20] Oetting, J. "A comparison of modulation techniques for digital radio." *IEEE Transactions on communications*, 27(12), 1979, pp. 1752-1762.

[21] IEEE Standard Association. "IEEE standard for local and metropolitan area networks part 15.6: Wireless body area networks." *IEEE Standard for Information Technology*, 2012, pp. 1-271.

[22] Recommendation. "Narrowband orthogonal frequency division multiplexing power line communication transceivers for G3-PLC networks." *ITU-T*, 2014.

[23] Galli, S., & Lys, T. "Next generation narrowband (under 500 kHz) power line communications (PLC) standards." *China communications*, 12(3), 2015, pp. 1-8.

[24] Lee, W. C. "The advantages of using repetition code in mobile radio communications." *36th IEEE Vehicular Technology Conference (VTC)*, 1986, pp. 157-161.

[25] Wikipedia. "Repetition code", https://en.wikipedia.org/wiki/Repetition_code, 2016.

[26] Wikipedia. "Majority logic detection", https://en.wikipedia.org/wiki/Majority_logic_de-coding, 2013.

[27] Han, S., and Choi, J. W. "Performance Analysis of 802.15.6 WBAN DPSK system." *한국통신학회 종합 학술 발표회 논문집 (하계)*, 2014, pp. 648-649.

[28] Couch, L. W., Kulkarni, M., and Acharya, U. S. *Digital and Analog communication systems*, Prentice Hall, 1997, 789 pages.

[29] NI USRP-292x/293x Datasheet, National Instruments, 2015.

[30] N9030A PXA X-Series Signal Analyzer Datasheet, Agilent Technologies, 2013.

[31] N5182A MXG Vector Signal Generator Datasheet, Agilent Technologies, 2006.

요 약 문

저전력 통신을 위한 반복 기법이 적용된 비동기 M-ary DPSK 수신기의 성능 분석

본 논문에서 우리는 저 전력 및 신뢰성 있는 통신을 위한 반복 기법이 적용된 비동기 M-ary DPSK 수신기의 성능을 분석한다. 비동기 DPSK 의 잘 알려진 특성은 수신 신호의 위상 동기화에 대한 필요가 없기 때문에, 동기 PSK 보다 저 복잡도 구현이 가능할 수 있지만, 수신기 성능은 더 나빠지게 된다. 강인한 검출 성능을 얻기 위해서 에러 정정 능력이 있는 반복 코드가 DPSK 와 함께 사용될 수 있다. 예를 들어, IEEE 802.15.6 WBAN 과 IEEE P1901.2 에서는 반복 기법과 함께 M-ary DPSK 변조가 사용된다. 그들은 bit spreader 와 bit interleaver 를 이용한 반복 방식을 고용한다. 반면에, 본 연구에서는 추가적인 성능 이득의 가능성을 찾기 위해서 비트 반복 대신에 심볼 반복이 고용된다. 구체적으로 말하자면 반복 방식과 함께 사용되는 비동기 M-ary DPSK 수신기의 에러율은 잡음 분포 모양에 영향을 받게 되고, 그것의 영향은 반복 차수에 따라 변화한다. 우리는 각각의 변조 차수에서 어떤 반복 차수가 주어졌을 때, 그때의 잡음 분포는 수신 신호가 에러 결정 경계 내에 더 많이 분포되도록 만들거나 에러 결정 경계 밖으로 더 많이 분포되도록 만드는 것을 확인하였다. 즉, 우리의 제안된 기법은 반복 기법이 적용된 비동기 M-ary DPSK 의 비트 오율을 낮추는 데 있어 도움이 될 수 있다. 추가적으로 단순히 심볼 반복을 고용하는 것 외에 신호 복조시에 추가적인 정보를 이용하여 더 높은 신뢰성을 얻을 수 있는 대안을 제시한다. 본 논문에서 우리는 시뮬레이션과 실험을 수행함으로써 심볼 반복이 적용된 비동기 M-ary DPSK 수신기의 성능을 규명하고, 이들의 에너지 효율을 최적화시킬 수 있는 반복 차수를 찾는다.

핵심어: 저전력 통신, 신뢰성, 비동기, 차동 위상 편이 방식, WBAN, 심볼 반복